AD___________________

Award Number: DAMD17-98-1-8608

TITLE: Therapeutic and Biologic Studies in a Murine Model of NF1

PRINCIPAL INVESTIGATOR: Kevin M. Shannon, M.D.

CONTRACTING ORGANIZATION: The University of California
San Francisco, California 94143-0962

REPORT DATE: October 2001

TYPE OF REPORT: Final

PREPARED FOR: U.S. Army Medical Research and Materiel Command
Fort Detrick, Maryland 21702-5012

REPORT DOCUMENTATION PAGE

Form Approved OMB No. 074-0188

1. AGENCY USE ONLY (Leave blank)	2. REPORT DATE	3. REPORT TYPE AND DATES COVERED
	October 2001	Final (23 Sep 98 - 22 Sep 01)

4. TITLE AND SUBTITLE
Therapeutic and Biologic Studies in a Murine Model of NF1

5. FUNDING NUMBERS
DAMD17-98-1-8608

6. AUTHOR(S)
Kevin M. Shannon, M.D.

7. PERFORMING ORGANIZATION NAME(S) AND ADDRESS(ES)
The University of California
San Francisco, California 94143-0962

E-Mail: kevins@itsa.ucsf.edu

8. PERFORMING ORGANIZATION REPORT NUMBER

9. SPONSORING / MONITORING AGENCY NAME(S) AND ADDRESS(ES)

U.S. Army Medical Research and Materiel Command
Fort Detrick, Maryland 21702-5012

10. SPONSORING / MONITORING AGENCY REPORT NUMBER

11. SUPPLEMENTARY NOTES
Report contains color

12a. DISTRIBUTION / AVAILABILITY STATEMENT
Approved for Public Release; Distribution Unlimited

12b. DISTRIBUTION CODE

13. ABSTRACT ***(Maximum 200 Words)***

This final report describes the outcome of a translational research project involving *Nf1* mutant mice with myeloid leukemia. Progress made during the full period of support is reviewed concisely and a final summary is provided. This research study pursued two Technical Objectives. First, the therapeutic efficacy of two agents (1) mycophenolate mofetiel (MM) and, (2) a fusion toxin that targets the GM-CSF receptor was examined. These compounds represent rational new approaches for treating NF1-associated tumors. MM has been tested in the mouse model and our preliminary data indicate that it is unlikely to provide benefit to NF1 patients. However, biochemical studies demonstrated the predicted inhibitory effects on signaling through downstream effectors of Ras-GTP. We produced and purified a GM-CSF immunotoxins and tested an number of these *in vitro*. These studies surprisingly revealed agonist (rather than inhibitory effects) of the conjugates. The investigators are continuing to develop improved reagents. In aim 2, utilized *Nf1* mutant mice to extend clinical observations suggesting that individuals with NF1 are susceptible to the development of therapy-associated second cancers. These studies demonstrated dramatic cooperation between heterozygous inactivation of *Nf1* and exposure to mutagens in cancer development.

14. SUBJECT TERMS	15. NUMBER OF PAGES
Neurofibromatosis, cancer	44
	16. PRICE CODE

17. SECURITY CLASSIFICATION OF REPORT	18. SECURITY CLASSIFICATION OF THIS PAGE	19. SECURITY CLASSIFICATION OF ABSTRACT	20. LIMITATION OF ABSTRACT
Unclassified	Unclassified	Unclassified	Unlimited

TABLE OF CONTENTS

(1)	Front Cover	page 1
(2)	Standard Form 298	page 2
(3)	Table of Contents	page 3
(4)	Introduction	pages 4-5
(5)	Body	pages 5-21
(6)	Key Research Accomplishments	page 21
(7)	Reportable Outcomes	pages 22-23
(8)	Conclusions	pages 23-24
(9)	References	pages 24-26
(10)	Figures	pages 27-41
(11)	Appendicies	attached
	Research Abstracts (2)	

INTRODUCTION

Individuals with neurofibromatosis type 1 (NF1) are predisposed to specific benign and malignant neoplasms including juvenile myelomonocytic leukemia (JMML). Clinical data also suggest that children with NF1 have an increased risk of developing leukemia as a complication of genotoxic therapies for another primary cancer (1). Genetic and biochemical studies of patient leukemias performed in our laboratories have shown that *NF1* functions as a tumor suppressor gene in immature hematopoietic cells by negatively regulating Ras signaling (2-6). Similarly, heterozygous *Nf1* mutant *(Nf1+/-)* mice show an increased incidence of myeloid leukemia and other cancers (7). We found that treatment with the alkylating agent cyclophosphamide cooperates strongly with heterozygous inactivation of *Nf1* in murine leukemogenesis (8). Homozygous *Nf1* mutant embryos *(Nf1-/-)* die *in utero.* Like human JMML cells, *Nf1-/-* fetal hematopoietic cells display a selective pattern of hypersensitivity to the cytokine growth factor GM-CSF in myeloid progenitor colony assays (5, 9). Adoptive transfer of these cells consistently induces a myeloproliferative disorder (MPD) that resembles JMML in irradiated recipients (9, 10). The predictable nature of this MPD, the fact that transplanted mice survive for many months, and the well-characterized biochemical alterations in *Nf1*-deficient hematopoietic cells make this model attractive for testing novel therapeutics and for biologic studies of growth control.

The approved Statement of Work for this translational research project listed two Technical Objectives, which we have pursued through two Specific Aims. Aim 1 proposed preclinical studies in recipient mice that have been transplanted with *Nf1*-deficient fetal liver cells to investigate the therapeutic efficacy of two agents (1) an inhibitor of *de novo* guanine nucleotide synthesis and, (2) a recombinant fusion toxin that targets the GM-CSF receptor. These compounds were chosen because they represent rational new approaches for treating NF1-associated tumors. We also proposed correlative biochemical studies to elucidate the effects of these therapeutics on cellular GTP levels and Ras signaling. In aim 2, we utilized *Nf1* mutant mice to extend clinical observations suggesting that individuals with inactivation of one *NF1* allele are susceptible to the development of therapy-associated second cancers. We exposed cohorts of wild type and *Nf1+/-* mice to cyclophosphamide or radiation therapy alone, or to radiation combined with cyclophosphamide, to test the hypothesis that these mutagens might cooperate with each other and with inactivation of *Nf1* in tumorigenesis. We have generated an extensive collection of tumor tissues that we are examining for loss of heterozygosity (LOH) at *Nf1*. We are performing additional correlative molecular and biochemical studies. The experiments performed under this award have yielded novel data that may be of practical value to patients with NF1 and their physicians.

BODY

Technical Objective (Aim) 1: Testing Rational Therapeutics in Nf1 Mice

Overview of Preclinical Therapeutic Studies. This component involved independently testing the efficacy of two rational therapeutic agents to inhibit the growth of *Nf1-/-* hematopoietic cells *in vivo,* and performing correlative biochemical and cell biologic assays. Our progress is presented below.

Preclinical Evaluation of Mycophenolate Mofetil (MM). As described in our proposal, MM is the morpholinoethyl ester of mycophenolic acid (MPA). MPA was first isolated from a fermentation of corn in 1898 by Gosio and is a non-competitive reversible inhibitor of eukaryotic inosine monophosphate dehyrogenase (IMPDH), which is required for *de novo* guanine nucleotide synthesis. MPA depletes GTP levels in human monocytes and lympohocytes *in vitro* at clinically attainable concentrations of 1-10 μM (11, 12). The rationale for investigating this agent in NF1-associated tumors is based upon the idea that therapeutics that reduce the amount of intracellular guanine might also lower the ratio of GTP to GDP in the cell. This, in turn, might decrease Ras-dependent growth because the activation state of Ras depends on the selective binding of GTP. The murine adoptive transfer model is ideal for studies that examine the efficacy of GTP reduction in inhibiting the abnormal growth of *Nf1*-deficient cells because the biochemical consequences of gene inactivation are well characterized in hematopoietic cells and because these cells rely heavily on the *de novo* pathway for nucleotide biosynthesis. Indeed, MM has shown anti-tumor efficacy in a number of preclinical studies performed in athymic nude mice. Additional background information, including calculations which suggested that cells in which an oncogenic *RAS* mutation or loss of *Nf1* would show enhanced sensitivity to a reduction in intracellular GTP concentrations, were presented in our proposal.

Summary of Progress in Years 1 and 2. During year 1, we determined that 400 mg/kg of MM was well-tolerated in wild-type mice, and we initiated studies in irradiated recipients engrafted with either *Nf1+/+* or *Nf1-/-* fetal liver cells. These studies surprisingly showed that recipients developed dramatic increases in total leukocyte and myeloid cell counts, which were more pronounced in mice engrafted with *Nf1-/-* cells.

We extended these studies in year 2. Leukocytosis was a consistent finding in mice treated with MM, with some *Nf1-/-* recipients showing white blood cell counts in excess of 100,000 per mm^3 (Fig. 1). Bone marrow smears and splenic tissue sections (Fig. 2) revealed striking myeloid hyperplasia. Spleen weights were greater in wild type recipients that received MM than in untreated controls, but not in *Nf1-/-* recipients (Fig. 3). Assays of bone marrow colony forming unit granulocyte macrophage (CFU-GM) numbers revealed a slight rise in splenic CFU-GM numbers from abnormally high baseline levels in a *Nf1-/-* recipients; however, wild type mice showed a highly significant increase (data not shown). Thus, accelerated myelopoiesis in MM-treated wild type mice is associated with the appearance of substantial numbers of splenic CFU-GM.

Biochemical Effects of MM Treatment. A major research question in the final year of the project involved determining if MM treatment reduced GTP levels in primary cells and, if this is true, how this altered Ras activation in resting and in growth factor-stimulated cells. We succeeded in adapting published methods to measure cellular GDP and GTP concentrations *in vitro*. However, multiple attempts to reliably quantify GTP and GDP levels in primary murine hematopoietic cells proved unsuccessful. It should be noted that there are no established methods in this area

As a surrogate for measuring cellular GTP and GDP levels, we interrogated downstream effectors of activated Ras, including Extracellular signal-regulated kinase (ERK; also known as MAP kinase) and protein kinase B (PKB; also known as Akt), a downstream effector of phosphoinositide-3-OH kinase (PI3K). ERK is an important regulator of proliferation and differentiation while PKB signaling strongly implicated as having anti-apoptotic effects in hematopoietic cells. These studies were initially undertaken in congenic *Nf1+/+* and *Nf1-/-* murine myeloid cells transfected with a retroviral vector which we constructed by inserting a truncated allele of the *c-Myb* oncogene into the murine stem cell virus (MSCV) backbone. When used to infect wild-type fetal liver cells, this virus efficiently generates pools of cells that retain many characteristics of primary myeloid progenitors and require growth factors for survival and proliferation (data not shown). *Myb*-transfected myeloid cells are maintained in media supplemented with GM-CSF. Cells were collected and incubated for 4 hours at 37°C in media without GM-CSF and with 0 μM, 0.5 μM, 1 μM, or 5 μM of MPA. Cells were then incubated for 7.5 minutes at 37°C with or without 10 ng/mL of recombinant murine GM-CSF. Cell lysates were run on a TGS gel and transferred to filter paper. Blots were probed with polyclonal anti-phospho-ERK and anti-ERK2 antibodies (Fig 4). Increasing concentrations of MPA blocked ERK activation without altering ERK protein levels. These data support the hypothesis that MPA decreases intracellular GTP-GDP ratio, and therby blunt the ability of growth factors to activate Ras. We next sought to confirm these findings *in vivo*.

Nf1+/+ and *Nf1+/-* mice were treated with control vehicle or MM at 400 mg/kg/day by gavage for 6 days, then sacrificed 4 or 24 hours after the last dose. Bone marrow was harvested with minimal handling and incubated at 37°C for 7.5 minutes with or without 10ng/mL of recombinant murine GM-CSF. Cells were treated as above, and an aliquot of lysate was similarly transferred and probed with polyclonal anti-phospho-ERK and anti-ERK2 antibodies (Fig. 5). As in *Myb*-transformed cells, treatment decreased ERK activation in response to GM-CSF. This effect abated by 24 hours; indeed, a rebound hyperstimulation was observed (Fig. 5). The effects of MM on signaling downstream of Ras were further interrogated using an assay in which PKB is immunoprecipitated from lysates and incubated with a GSK-3b fusion protein at 30°C for 30 minutes. This lysate was then run on a TGS gel, transferred and probed with an anti-phospho-GSK-3b antibody (Fig 6). MM treatment decreased PKB kinase activity, presumably because of decreased Ras-GTP levels upstream of the PI3 kinase-PKB pathway.

<u>Preclinical Evaluation if a DT_{ct}GM-CSF Recombinant Fusion Toxin</u>. Studies of myeloid progenitor colony growth in JMML patients and *Nf1-/-* mice have implicated hypersensitivity to GM-CSF in leukemogenesis. In a previous study, we crossed lines of *Nf1* and *Gmcsf* mutant mice, and transferred doubly mutant fetal liver cells into irradiated wild type or *Gmcsf*-deficient recipients (13). Genetic ablation of GM-CSF production in host bone marrow and in donor fetal liver cells markedly attenuated the JMML-like MPD. Furthermore, adoptive transfer of doubly mutant bone marrow cells with established disease into secondary *Gmcsf-/-* recipients reversed the MPD, which could be reinduced by treatment with exogenous recombinant murine GM-CSF. These data implicate GM-CSF hypersensitivity as playing a central role in JMML (13). Recent experiments in which we crossed *Nf1* mutant mice with a line that has inactivated the β chain of the GM-CSF receptor provide further support for this hypothesis (data not shown). These studies suggest that inhibiting this signaling pathway might provide therapeutic benefit.

<u>Summary of Progress in Years 1 and 2</u>. A major goal of Technical Objective 1 involved producing a highly purified recombinant DT_{ct}GM-CSF fusion toxin and using this novel re agent to perform *in vitro* and *in vivo*

studies with the goal of specifically delivering the diphtheria toxin to myeloid cells via the GM-CSF receptor. Given emerging evidence suggesting that aberrant expression of growth factor receptors may underlie other pathogenic complications of NF1 (14), this general therapeutic approach has borad implications. As summarized in previous Progress Reports, Dr. Perentesis produced and purified substantial amounts of the murine DT_{ct}GM-CSF fusion toxin for *in vivo* murine studies. The initial *in vitro* characterization of this molecule revealed high level production and >95% purity of a monomeric protein with the expected molecular mass of molecular mass of ~57 kDa as deduced from the nucleic acid sequence of DT_{ct}GM-CSF. The final product of TSK-gel G2000 purification is estimated to exceed 98% purity. The integrity of expression of both the diphtheria toxin and GM-CSF moieties of DT_{ct}GM-CSF was confirmed in immunoblot analysis employing antisera to diphtheria toxin.

Dr. Shannon's laboratory used this material to perform a series of experiments during year 2 to test the ability of this fusion molecule to inhibit the growth of cultured cell lines and of primary murine bone marrow cells. WEHI-3 cells were selected for the first series of studies because we previously found that this cell line expresses surface GM-CSF receptors and dramatically up-regulates MAP kinase activity in response to GM-CSF (data not shown). Surprisingly, the DT_{ct}GM-CSF had no demonstrable effects on the growth of WEHI-3 cells under a number of culture conditions (data not shown). To further address the biologic activity of the fusion toxin, primary mouse bone marrow cells were plated in methylcellulose cultures containing various concentrations of GM-CSF and DT_{ct}GM-CSF immunotoxin. The results of these experiments are summarized in Figure 7. We observed no inhibitory effect of DT_{ct}GM-CSF on CFU-GM colony formation. Indeed, the immunotoxin demonstrated significant agonist activity; that is, DT_{ct}GM-CSF induced colony formation in a dose-dependent manner (Fig. 7). These results, which were confirmed with multiple lots of DT_{ct}GM-CSF, are consistent with the ability of the GM-CSF moiety of the recombinant fusion protein to recognize and bind the GM-CSF receptor. However, we did not detect the cytotoxic effects that we had expected from targeting diptheria toxin to the GM-CSF receptor. Based upon these initial results, Dr. Perentesis instituted major refinements in the expression and purification method for DT-mGMCSF during year 3 in an effort to overcome problems with product stability and activity. These studies are described in the following sections

Production of DT_{ct}GM-CSF Immunotoxin. During the first 2 years of this project, Dr. Perentesis accomplished a number of goals including: (1) design and construction of the recombinant diphtheria toxin - murine granulocyte-macrophage fusion toxin expression vector, PET-11d-DT-mGMCSF; (2) evaluation of methods for expressing the recombinant fusion toxin, DT-mGMCSF; (3) *in vitro* characterization and confirmation of the protein structure of DT-mGMCSF by polyacrylamide gel and western immunoblot analyses; (4) *in vitro* confirmation of the characteristic diphtheria toxin ADP-ribosyltransferase activity of DT-mGMCSF; and (5) preliminary assays of the *in vitro* cytotoxic activity of the fusion toxin. These studies were presented in detail in previous Progress Reports. The preliminary assays of *in vitro* toxicity revealed that DT-mGMCSF had lost cytotoxic activity after extended storage at the University of Minnesota and transfer to Dr. Shannon's laboratory at UCSF (see Fig. 7 above). During the final year of this project, substantial effort was devoted to the design and evaluation of multiple new techniques for the purification of DT-mGMCSF to increase stability and insure that it assumes native conformation after production. These purification refinements primarily focused on the development of novel refolding methods for the recombinant fusion toxin and are detailed below.

Dr. Perentesis also designed and constructed several new diphtheria toxin-GMCSF expression vectors to provide another modality to overcome the obstacles associated with conformational folding and stability of the recombinant fusion toxin. These new expression vectors, pMAL-2cx-DT-mGMCSF and CBDintein-DT-mGMCSF add a unique molecular "tag" to the fusion toxin that can be recognized by a tag-specific affinity column to increase the efficiency purification. With these new expression constructs, extracts of bacterial cell lines producing the fusion toxin are applied to the tag-specific affinity column resulting in retention of the fusion toxin, and other unwanted cellular proteins are removed in the column flow-through. Subsequently the fusion toxin is eluted from the affinity column. The molecular tag is linked to the fusion toxin by a unique peptide sequence that can be recognized by a highly specific protease (e.g. activated factor Xa). Purified fusion protein is then produced by removal of the purification tag by incubation with the specific protease. Subsequent high performance chromatography steps are then employed to remove the protease and tag, resulting in high specific purity of the final fusion toxin product. Final steps in production include endotoxin removal. Significant effort in this funding period was also expended in the optimization of the purification procedures for the novel expression vectors.

Methods for Improved Renaturation and Refolding of DT-mGMCSF Expressed from PET-DT-mGMCSF. High level expression of DT-mGMCSF from *E. coli* containing pET-11d-DT-mGMCSF expression vectors was conducted using techniques optimized in Dr. Perentesis' laboratory. All manipulations of *E. coli* bearing intact recombinant fusion toxin were performed under modified Biosafety Level 3 (BL3) containment practices. *E. coli* strain HMS174(de3)plysS transformed with pET11d-DT-mGMCSF was grown at 37°C in LB medium with carbenicillin (50 µg/ml) to an absorbance (Å595) of 0.55-0.65. Expression of the fusion gene was induced by the addition of isopropyl-B-D-thiogalactopyranoside (IPTG) to a final concentration of 0.5 mM. The bacterial cells were collected by centrifugation after one hour of induction.

Over the past year, Dr. Perentesis developed and studied several new methods for improved renaturation and refolding of DT-mGMCSF (see overview in Figure 8). This included a new common framework "basic refolding method" for production and renaturation, and several modifications of this method. In the "basic refolding method," the bacterial pellets were resuspended in 0.1 culture volumes of Wash Buffer (20 mM Tris-HCl, pH 7.5, 10mM EDTA, 1% Triton X-100). Cells were lysed by adding lysozyme to a final concentration of 100 µg/ml and incubated at 30°C for 15 minutes and sonicated on ice 3 x 30 seconds pulses. Following cell lysis, protease inhibitor was added. Inclusion bodies were collected by centrifugation at 10,000 g for 10 min at 4°C. The pellet was then washed twice with wash buffer. The pellet containing the inclusion bodies was weighted and resuspended in solubilization buffer (50 mM CAPS, pH 11, 0.3% N-lauroylsarcosine, 1 mM DTT) at a concentration of 10-20 mg/mL. After 15 minutes incubation at room temperature, the sample was clarified by centrifugation at 10,000 g for 10 min at room temperature. The supernatant containing the solubilized protein was dialyzed against Dialysis Buffer (20 mM Tris-HCL, pH 8.5, 0.1 mM DTT, 50 mM NaCl) for 2 x 3 hours at 4°C. The sample was then dialyzed trough 2 more changes of 3 hours each against the dialysis buffer lacking DTT. The sample was filtered and subjected to mono-Q sepharose high performance liquid chromatography (HPLC) column.

A variety of modifications to the basic refolding method for renaturation and refolding were also evaluated. These modifications included multiple studies examining the effect of the addition of non-detergent sulfobetaines (NDSB) in the dialysis buffer to reduce protein aggregation and improve refolding and attainment of native protein conformation. The following NDSB were used: NDSB 201, NDSB 195, and NDSB 256 at a final concentration of 1M.

Purified samples of DT-mGMCSF were analyzed with SDS-PAGE and immunoblot, and ADP-ribosylation assays. Sodium dodecyl sulfatepolyacrylamide gel electrophoresis (SDS-PAGE) and Phototope-HRP Western blot analyses using goat diphtheria antitoxin (anti-DT; Bethyl) antibodies were performed by standard methods using 10% gels in a Mini-Protean II gel apparatus (Bio-Rad). Diphtheria toxin standards were obtained from Sigma. Primary antibodies were used at a dilution of 1:5000 for diphtheria antitoxin, and a dilution of 1:10000 for anti-MBP antibody. Secondary antibodies, rabbit anti-goat (Bethyl laboratories), covalently linked to horseradish peroxidase, were used at a 1:7500 dilution. HRP-linked anti-rabbit IgG (Cell Signaling Technology) at 1:2000 dilution and HRP-conjugated anti-biotin antibody at 1:1000 dilution. The characteristic ADP-ribosyltransferase activity of the diphtheria toxin moiety of samples of the DT-mGMCSF fusion toxin was measured and compared to standards of native diphtheria toxin. HPLC column fractions containing intact DT-mGMCSF fusion toxin were pooled and then concentrated by Amicon filtration. The ADP ribosylation reaction was initiated by adding 500ng of purified fusion protein to a reaction mixture containing 20mM Tris-HCl pH 7.5, 1mM EDTA, 50mM DTT, eukaryotic elongation factor 2 (rabbit reticulocyte lysate), and ^{32}P-NAD(1×10^6cpm). The ADP-ribosyltransferase reaction was conducted at 37°C for 15 minutes and terminated by adding 20% TCA. Precipitated protein containing elongation factor 2 with incorporated radioisotope was collected by filtration on nitrocellulose membranes, with a ice cold 5% TCA wash and cold 95% ethanol wash. Radioisotope incorporation and ADP-ribosyltransferase activity was measured by liquid scintillation counting.

The analysis of these different methods for improved DT-mGMCSF recombinant fusion toxin expression and renaturation revealed production and >98% purity of a monomeric protein with a molecular mass of ~57 kDa, the expected molecular mass of DT-mGMCSFas deduced from its nucleic acid sequence (Fig. 9). The integrity of expression of both the diphtheria toxin and GMCSF moieties of DT-mGMCSF was confirmed in immunoblot analysis employing antisera to diphtheria toxin. The levels of ADP-ribosylation activity were substantially higher when using the new "basic refolding method" for protein refolding developed in this grant cycle when compared with previous methods (data not shown). In investigations of further modification of the "basic refolding method" for renaturation, Dr. Perentesis also demonstrated that activity of DT-mGMCSF was not enhanced by the addition of non-detergent sulfobetaines. The DT-mGMCSF production lots with the highest specific activity will be assessed for specific cytotoxicity using *in vitro* murine bone marrow colony forming unit assays prior to murine *in vivo* studies. Additional funding has been secured by Dr. Perentesis to complete these investigations.

Design and Construction of Alternate Expression Vector pMAL-2cx-DT-mGMCSF and CBD-intein-DT-mGMCSF. The new expression constructs produced in this funding period (pMAL-2cx-DT-mGMCSF and CBD-intein-DT-mGMCSF) were developed using the framework DT-mGMCSF genetic cassette from the parent plasmid PET-11d-DT-mGMCSF. In the parent plasmid PET-11d-DT-mGMCSF the polymerase chain reaction (PCR) had been employed for mutagenesis of the diphtheria toxin gene to delete the coding region for the native toxin binding domain, and provide coding sequences for a translation initiation ATG codon, a seven residue linker segment for fusion with the GMCSF gene, and convenient flanking NcoI restriction enzyme sites for cloning.

An overview of the construction of expression vector pMAL-2cx-DT-mGMCSF is shown in Figure 10. The polymerase chain reaction (PCR) was used for mutagenesis of the DT-mGMCSF gene (using pET-11d-DT-mGMCSF as a template) to add BamHI restriction enzyme cleavage sites to both 5' end and 3' end. The PCR primers for DT-mouse GMCSF inculded a 5'promer(5'-ACCATGGGATCCGATGATGTTGTTGAT-3') and 3' primer (5'-GGGGATCCTCATTTTTGGACTGG-3'). DNA fragments amplified by the polymerase chain reaction (PCR) were initially cloned into the TA cloning vector as directed by the manufacturer (Invitrogen). Plasmid DNAs were prepared by using Qiaprep spin miniprep kit (Qiagen).

Dr. Perentesis also constructed expression vector CBD-intein-DT-mGMCSF to produce recombinant DT-mGMCSF . PCR was used for mutagenesis of the DT-mGMCSF gene to add NdeI and EcoRI restriction enzyme sites to 5' and 3' terminii respectively. The PCR primers for the fusion toxin gene included a 5' primer (5'-TACATATGGGCGCTGATGATGTTGTTG-3') and 3' primer (5'-GGGGATCCGAATTCTTGGACTGG-3'). DNA fragments amplified by the polymerase chain reaction were initially cloned into the TA cloning vector as directed by the manufacture (Invitrogen). Plasmid DNAs were prepared by using Qiaprep spin miniprep kit (Qiagen). The fusion toxin gene cassette was finally constructed into NdeI and EcoRI sites of pTYB2 vector (DT-mGMCSF positioned at the 5' end of intein gene) and pTYB12 vector (DT-mGMCSF positioned at the 3' end of intein gene).

Cloning strategies and other genetic manipulations were positioned to assure maintenance of the translational reading frame, and fidelity of PCR amplification and genetic constructions were confirmed by DNA sequencing. Oligonucleotide primers were synthesized with an Applied Biosystems 394 DNA synthesizer at the University of Minnesota Microchemical Facility. Plasmid DNAs were prepared by use of the Wizard DNA purification resin (Promega, Madison, WI). DNA fragments amplified by the polymerase chain reaction (PCR) were initially cloned into the pT7Blue vector as directed by the manufacturer (Novagen), with DNA sequencing confirmation by the dideoxy method of Sanger using CircumVent thermal cycling reagents (New England Biolabs, Beverly, MA). Restriction endonucleases, Taq DNA polymerase, and T4 DNA ligase were procured from BRL-Life Technologies (Gaithersburg, MD), Promega, New England Biolabs, or Perkin Elmer (Norwalk, CT), and used according to the specifications directed by the manufacturer. Standard techniques were employed for other manipulations of DNA including agarose gel electrophoresis, isolation and purification of restriction endonuclease fragments, cloning, and plasmid transformation into bacteria.

Expression and Purification of DT-mGMCSF from *E.coli* Containing pMAL-2cx-DT-mGMCSF Expression Plasmids. Dr. Perentesis also investigated the use of the new pMAL-2cx-DT-mGMCSF expression plasmids as an alternative method for the production of DT-mGMCSF with an intact conformation. *E. coli* HMS174(de3)plysS transformed with pMAL-2cx-DT-mGMCSF was grown at 37°C in LB medium with carbenicillin (50 μg/ml) to an absorbance (Å595) of 0.55-0.65. Expression of the fusion gene was induced by the addition of isopropyl-B-D-thiogalactopyranoside (IPTG) to a final concentration of 0.3 mM. The bacterial cells were collected by centrifugation after two hour of induction. The bacterial pellets were then resuspended in column buffer (20mM Tris-HCl/1mM EDTA/200mMNaCl pH 7.4), and frozen in a dry ice-ethanol bath and stored at –20°C. Lysis of the cells was achieved by thawing cell suspension in iced-water and sonication in 6 short pulses of 15 seconds each. A crude extract containing the recombinant fusion toxin was obtained by centrifugation at 9000 x g for 30 minutes. The supernatant was filtered and diluted 1:3 with column buffer, prior to mixing it with amylose resin and incubation for 18 hours at 4°C. The amylose resin and sample were then poured into a 2.5 x 10 column, which was then washed with 12 column volumes of column buffer and eluted with column buffer and 10 mM maltose. The final eluant was concentrated to approximately 3-5 ml and protein concentration was determined by the Bradford protein assay (Bio-Rad).

The MBP moiety was cleaved from the MBP-DT-mGMCSF fusion by incubation with Factor Xa at a w/w ratio of 1% the amount of fusion protein. The reaction mixture was incubated for 18 hours at 4°C. SDS-PAGE analyses were used for confirming completion digestion. Dialfiltration, Q-sepharose column and amylose affinity column were used to further separate MBP (maltose binding protein) and DT-mGMCSF. We found that use of this expression vector results in the high level expression of recombinant MBP-DT-mGMCSF fusion. Current activities are directed to the evaluation of the following 3 methods for further purification:

Method 1. The MBP portion of the fusion is cleaved by incubation with Factor Xa at a w/w ratio of 1% the amount of fusion protein. The reaction mixture is incubated for 18 hours at 4°C. Separation of DT-mGMCSF from MBP is effected with HPLC using a Q-sepharose column and eluted with a linear salt gradient from 0.05-0.5M NaCl in 20mM Tris pH 7.8 at room temperature, and in separate experiments, at 4°C.

Method 2. After elution from the amylose column, HPLC using a Q-sepharose column is employed to eliminate the contaminating proteases from the *E. coli* extract with gradient conditions as outlined above. The MBP- DT-mGMCSF containing elutant is concentrated and incubated with Factor Xa at a w/w ratio of 1% the amount of fusion protein. The reaction mixture is incubated 18 hours at 4°C. The MBP and DT-mGMCSF proteins are separated by loading the sample into an amylose column and collected in the flow through.

Method 3. After eluting from the amylose column, cleavage of MBP is conducted using the same techniques described in Method 1. The resulting sample containing maltose, MBP and DT-mGMCSF is then dialyzed against citrate phosphate buffer (20mM citrate phosphte buffer, 50 mM NaCl PH: 6.5). The sample is then concentrated prior to be loaded into a CM Biogel A column (cation Column). Elution conditions include a citrate buffer with 0.4mM Na Cl PH:6.5.

The DT-mGMCSF production lots with the highest specific activity will be assessed for specific cytotoxicity using *in vitro* murine bone marrow colony forming unit assays prior to murine *in vivo* studies. Additional funding has been secured by Dr. Perentesis to complete these investigations. An overview of studies in progress for the expression and purification of DT-mGMCSF from CBD-intein-DT-mGMCSF expression plasmids is shown in Figure 11.

Technical Objective (Aim) 2: Chemotherapy and Radiation Studies

Overview. These studies were founded upon clinical observations suggesting that children with NF1 are at increased risk of developing myeloid and other tumors after being treated with multi-modal therapy for another cancer (1). These human data implicated exposure to alkylating agents in the development of therapy-related leukemia (t-ML). Based on these clinical findings and on the 10% risk of leukemia in untreated *Nf1+/-* mice (7), we previously exposed *Nf1+/-* mice to mutagenic agents frequently used to treat malignancies in patients with and without NF1 (15). We found that treating heterozygous *Nf1* mice with cyclophosphamide (CY), a commonly-used chemotherapeutic agent, markedly increased the incidence of myeloid malignancies and shortened the latency to disease onset. In this study, CY treatment was associated with the development of a myeloid disorder in 16 of 37 *Nf1+/-* mice, but in only 2 of 30 wild-type animals. Most affected mice developed MPD; this was frequently associated with loss of heterozygosity (LOH) involving the wild-type *Nf1* allele in 129/Sv mice but with a low incidence in the F1 129/Sv x C57BL/6 background. Cytogenetic analysis of bone marrow and spleen cells from mice with leukemia revealed a normal karyotype. To ascertain if LOH on Southern blots was associated with submicroscopic deletions of *Nf1* or with duplication of the mutant allele, we used a genomic *Nf1* probe from the disrupted segment of the gene to perform fluorescence *in situ* hybridization (FISH) analysis of hematopoietic cells from 3 mice. FISH revealed two structural copies of *Nf1* in each case, a result that is consistent with the pattern of allele loss in bone marrow cells from children with NF1 (K. Stephens, MM Le Beau, and KMS; unpublished data). The cytogenetic and FISH experiments were performed by Dr. Michelle Le Beau (University of Chicago). Preliminary data from these studies were presented in our original application and a paper has been published (8).

This *in vivo* model of t-ML has a number of novel features that facilitate basic and translational research studies of this important clinical disorder. First, the fact that *Nf1* mice recapitulate clinical observations made in NF1 patients suggest that this model will be relevant for understanding specific aspects human t-ML. Second, *Nf1* provides a genetic target to examine the mechanism(s) of alkylator-induced DNA damage in hematopoietic cells. Finally, this model allowed us to undertake controlled experiments that are neither feasible nor ethical in humans. In this project, we exploited this system to ask if radiation therapy, alone and in combination with CY, accelerates tumorigenesis in heterozygous *Nf1* mice. This question is highly relevant to the care of individuals with NF1 because radiation therapy is used frequently to treat NF1-associated tumors. Indeed, our initial data led the Children's Cancer Group to modify the treatment of children with NF1 who develop brain tumors so that they are not assigned to alkylator-intensive regimens. We have collected a large series of tumors from *Nf1* mutant mice treated with radiation and/or CY that we are using for molecular analysis. We are also examining the incidence of hypoxanthine guanine phosphoribosyl transferase *(Hprt)* mutations as an *in vivo* measure of DNA damage.

Summary of Progress in Years 1 and 2. In year 1, we escalated the dose of CY and found that F1 C57BL/6 x 129/Sv mice tolerate a curse of 200 mg/kg/week for 6 weeks, and consistently develop neutropenia. We next showed that we could administer a single 2 or 3 Gray (Gy, which is equivalent to 200 or 300 rads) dose of total body irradiation as a single fraction two weeks after the last dose of CY. The use of total body irradiation insures that all of the blood-forming marrow is exposed, and previous data have shown that 2-3 Gy is more leukemogenic than higher or lower doses in susceptible mouse strains (16). We found that *Nf1+/-* 129Sv x C57BL6 F1 mice tolerated these treatment regimens well with no deaths occurring during or after the radiation phase of the study. In these pilot studies, treatment was associated with a variable degree of leukopenia and anemia, depending on the regimen used (see below). Based on these results, we compared four groups of mice (1) CY + 3 Gy, (2) CY alone, (3) irradiation alone, and, (4) no treatment. In order to minimize the number of animals treated, the design included entering fewer mice in the control and CY alone arms because we have already ascertained the incidence of myeloid diseases in these cohorts. We began enrolling mice in July 1999 and entered 42 by the end of year 1. In year 2, we completed enrollment to a total of 192 mice. We monitored the entire cohort regularly during years 2 and 3 including visual inspection as well as serial blood counts.

Characteristics of Study Mice. The 192 C57Bl/6 x 129/Sv mice have now been monitored for 15 months from the end of the eight week treatment phase. These mice included 106 wild-type and 86 *Nf1+/-* mice which were assigned to one of four treatment groups: no treatment, CY 200 mg/kg/wk IP x 6 doses, 3 Gy irradiation, or sequential CY followed radiation at the same doses (Table 1). The mice tolerated the treatment well, with only two presumed treatment related mortalities occurring approximately three weeks following completion of treatment with CY and irradiation. The total white blood cell counts, absolute neutrophil counts, and hemoglobin levels declined in response to CY, and recovered following completion treatment. Furthermore, administration of radiation delayed the onset hematologic recovery in CY-treated animals (data not shown). Blood counts normalized by three weeks following completion of treatment. Serial blood counts from treated mice show that CY and RT at these doses produced moderate leukopenia and anemia when given alone, and that the sequential administration of CY followed by RT delays recovery of these counts (data not shown).

Table 1
Number of Mice Assigned to Each Treatment Group

Treatment Group	*Nf1+/+*	*Nf1+/-*
Untreated Control	20	12
CY	17	14
RT	32	31
CY+RT	37	29

Exposure to RT Increases the Risk of Death. Mice were monitored for evidence of disease, including obvious tumors, pale feet suggestive of anemia, decreased activity level, abnormal gait, or tachypnea. At this writing, 163 of 192 (85%) have either died or been sacrificed. The data presented here and in the following sections are based on interim analyses of these 163 animals. Kaplan-Meier analysis demonstrates that, when compared to wild-type mice, *Nf1+/-* mice show an increased risk of death in the untreated (p=0.0006), RT (p<0.0001), and CY+RT (p=0.0021) groups, but not in the CY group (p=0.2269)(Fig. 12). Among *Nf1+/-* mice, exposure to RT decreases the median survival from 440 days for untreated animals to 402 days (p=0.0957) for RT alone, and to 364 days (p=0.0878) for CY+RT. This increased risk of death does not reach statistical significance in *Nf1+/-* mice, which may be due to the outcome of the small, untreated control group, which is worse than expected based on our historical controls (Fig. 12). Consistent with this prediction, the CY-treated *Nf1+/-* mice fared better than untreated mice, and the RT and CY+RT treated *Nf1+/-* mice display a statistically significant increased risk of death when compared to CY-treated mice (p=0.0082 and p=0.0085, respectively, unadjusted for multiple comparisons).

Tumor Formation in *Nf1+/-* Mice. Most of the premature deaths were due to malignant neoplasms. At sacrifice, evaluation includes gross examination of external features and internal organs, and microscopic evaluation of internal organs. We carefully evaluate the blood and bone marrow of all mice and obtain blood counts using a Hema-Vet blood cytometer in our laboratory.

Approximately half of all wild-type and *Nf1+/-* mice develop pulmonary nodules, typically measuring 1.5 to 4 mm in diameter, histologically adenomatous, and usually noted at necropsy following the fifteen month observation period or at time of sacrifice for another tumor. These nodules did not cause morbidity and were excluded from the subsequent analysis. Included in the analysis, however, are five cases of lung cancer where the mouse developed moderately large pulmonary tumors (either >0.10 g or >5 mm in diameter) associated with either tachypnea, decreased activity, or physiologic polycythemia (Hgb > 15).

A preliminary evaluation of the first 163 mice revealed 71 mice with a malignancy. Tumor types observed to date have included myeloid leukemia, sarcoma, pheochromocytoma, lymphoma, adenocarcinoma of the lung, and Harderian gland tumors. Kaplan-Meier analysis, shown in Figure 13, demonstrated that exposure to CY+RT cooperates with *Nf1* in decreasing the latency and increasing the incidence of development of cancer. Furthermore, Table 2 depicts the cumulative proportion of mice that develop a malignacy following the assigned treatment and shows that most treated *Nf1+/-* mice developed cancer. These data are consistent with epidemiologic and biochemical studies that support the role of *Nf1* as a tumor suppressor.

Table 2
Cumulative Proportion of Mice Developing a Malignancy

	Nf1+/+	*Nf1+/-*
Untreated Control	1/17 (6%)	5/9 (56%)
CY	2/17 (12%)	7/11 (64%)
RT	9/27 (33%)	19/23 (83%)
CY+RT	7/34 (21%)	21/25 (84%)
Total	19/95 (20%)	52/68 (76%)

RT Cooperates with *Nf1* Heterozygosity in the Development of Secondary Malignant Myeloid Neoplasms. Thirty percent of the cancers observed were myeloid maligncies, most of which occurred in *Nf1+/-* mice (Table 3). Although there are no differences in the Kaplan-Meier analysis of the four *Nf1+/-* treatment groups, (p=0.5853 by logrank test), *Nf1+/-* mice demonstrated an increased risk of leukemia following RT when compared to their wild-type counterparts. Specifically, 4/27 (15%) wild-type versus 9/23 (39%) *Nf1+/-* animals developed myeloid disease (p=0.0019, logrank test). Three additional *Nf1+/-* mice treated with RT alone developed massive splenomegaly (>1g) and died without an adequate necropsy. Although these mice did have other features suggestive of myeloid disease, the reasons for their morbidity and mortality were not fully evaluable; therefore, they were censored at the time of their death. Assigning a diagnosis of a myeloid malignancy to these three mice would increase the proportion of irradiated *Nf1+/-* mice that developed a malignant myeloid disorder from 39% to 46%. The cumulative proportion of mice developing leukemia according to treatment group is shown in

Table 3. The myeloid disorders observed encompass a broad phenotypic spectrum including hypoplasia, myeloproliferation, and myeloid leukemia, all with varying degrees of dysplasia.

Table 3
Proportion of Mice Developing Myeloid Malignancies

	Nf1+/+	*Nf1+/-*
Untreated Control	0/17	2/9 (22%)
CY	0/17	2/11 (18%)
RT	4/27 (15%)	9/23† (39%)
CY+RT	0/34	4/25 (15%)

†excludes 3 cases of massive splenomegaly

Irradiated *Nf1*+/- Mice Develop Features of Myelodysplasia. In addition to increasing the risk of myeloid malignancies, RT also altered the spectrum of disease observed. Whereas untreated and CY exposed *Nf1*+/- mice developed MPD, mice treated with RT frequently showed features of myelodysplastic syndrome (MDS) that was not observed in non-irradiated mice. The dysplasia typically involved the granulocyte lineage while sparing the erythocyte and thrombocyte lineages. MDS was characterized by marked pancytopenia, preserved marrow cellularity, and moderate splenomegaly wth spelnic inflitration by myeloid cells capable of forming colony units-granulocyte macrophage (CFU-GM) in methylcellulose. Because no animal model of MDS has been reported, these data will be useful for describing the characteristics of secondary MDS in mice and provide the foundation for a classification scheme for future studies in this and other mouse models.

RT Cooperates with CY to Induce of Sarcomas in *Nf1*+/- Mice. Approximately 39% of SMNs occurring in *Nf1*+/- mice in this study were either sarcomas or pheochromocytomas, two tumor types typically associated with NF1. In contrast to myeloid leukemia, we observed a clear cooperative effect of exposure to CY+RT and *Nf1* inactivation in sarcomagenesis. A statistically significant increased incidence occurs in mice treated with CY or CY+RT; however, RT alone did not significantly alter this risk (Fig. 14). The cumulative proportion of mice developing sarcomas is shown in Table 4. We are currently exploiting banked tissues from these studies to investigate the genetic and biochemical lesions that contribute to tumorigenesis.

Table 4
Proportion of Mice Developing Sarcoma or Pheochromocytoma

	Sarcoma		Pheochromocytoma	
	Nf1+/+	*Nf1+/-*	*Nf1+/+*	*Nf1+/-*
Untreated Control	0/17	0/10	0/17	2/10 (20%)
CY	0/17	2/11 (18%)	0/17	1/11 (9%)
RT	0/27	3/26 (12%)	1/27 (4%)	2/26 (8%)
CY+RT	0/34	8/25 (32%)	0/34	2/25 (8%)

Representative hematoxylin and eosin (H&E) staining of these tumors revealed fascicles of spindle shaped cells with frequent mitotic figures characteristic of soft tissue sarcomas (Fig. 15). Although sarcomas are common in *cis Nf1-;p53-* mutant mice (17, 18), they are not increased in singly mutant heterozygous *Nf1* mice (7). In contrast, both human NF1 patients and *Nf1+/-* mice are predisposed to pheochromocytoma. Consistent with these observations, we identified pheochomocytomas in a low precentage of *Nf1+/-* mice. Exposure to RT and/or CY had no apparent effect on the incidence of pheochromocytoma (Table 4).

Hprt Assay. Hypoxanthine guanine phosphoribosyl transferase (HPRT) is a cellular enzyme crucial in the metabolism of the chemotherapeutic agent thioguanine into deoxythioguanine triphosphate, which can then be incorporated into DNA and cause cell death. Lymphocytes that have inactivated *Hprt* acquire the ability to proliferate in the presence of 6-thioguanine because they are unable to convert this drug to its active metabolite. *Hprt* mutation rate has been used as a surrogate marker for DNA damage induced by mutagenic compounds such as CY and irradiation, and for evaluating potential chemoprotective compounds (19, 20). However, it is not known if reducing the frequency of *Hprt* inactivation will correlate with a decrease in the risk of therapy-related cancer *in vivo.* If this proves true, *Hprt* could be used as a surrogate marker to test the mutagenic potential of new chemotherapeutic agents and of specific regimens.

We established the *Hprt* assay in our laboratory using published methods (19). *Hprt* mutation frequency is measured in male mice because this locus is on the X chromosome. We initiated these studies in C57BL6/129Sv mice treated with CY at a dose of 200 mg/kg/week for either 1 week (single dose) or for 6 weeks. The mice are sacrificed and splenocytes are isolated 55-60 days after the last drug dose. Preliminary data from a cohort of mice treated for 1 week showed a greater than 10 fold increase in the mutation frequency of CY-treated mice compared to controls (mutation frequency = 4.7×10^{-5} in CY-treated mice vs. 3.3×10^{-6} in the controls; $p = 0.038$). In a study supported by the American Cancer Society, we are testing the chemopreventive agent amifostine in CY-treated *Nf1* mice. As shown in Figure 16, amifostine markedly reduced the *Hprt* mutation rate in mice that received a single dose of CY, but was associated with a paradoxical increase in mutation rates after a full 6 week course. Consistent with this, our preliminary data suggest that amifostine does not protect *Nf1* mice treated with CY for 6 weeks from leukemia. In experiments that are currently in progress, we are comparing *Hprt* mutation rates in control mice with the rates in mice treated with CY alone, CY + radiation, or radiation alone.

We have also successfully adapted the protein truncation method that we have used to detect *NF1* mutations in human leukemias to analyze the murine homolog. This assay will prove useful for analyzing tumor tissues from our cohort that do not show LOH for somatic mutations in the wild-type *Nf1* allele.

KEY RESEARCH ACCOMPLISHMENTS

- Developed breeding stocks of mouse strains and generated recipients repopulated with *Nf1-/-* or wild-type fetal liver cells.
- Completed *in vivo* studies of MM in transplant recipients.
- Performed correlative biochemical studies of tissues from MM-treated mice.
- Produced DT_{ct}GM-CSF, and tested this compound *in vitro.*
- Devised improved process for producing and evaluating DT_{ct}GM-CSF
- Bred, genotyped, enrolled, and treated a cohort of 192 wild-type and *Nf1* mutant mice and demonstrated a cooperative effects between Nf1 inactivation and mutagen exposure in tumorigenesis.
- Developed novel models of RT-induced MDS and of RT and chemotherapy-induced sarcoma.
- Generated 8 cell lines from mouse tumors, including 5 from sarcomas, for genetic and biochemical studies.
- Established *Hprt* and protein truncation assays.

REPORTABLE OUTCOMES

(a) Review Article

Weiss B, Bollag G, Shannon KM. Hyperactive Ras as a therapeutic target in neurofibromatosis type 1. *Am J Med Genet* 1999; 89: 14-22.

(b) Abstracts

Weiss, BD, Lee D, Feldmann A, Aiyigari A, Shannon KM. Myeloproliferation in wild-type and Nf1 mutant mice treated with mycophenolate mofetil. Selected for presentation at the 2001 Meeting of the American Society of Hematology, Orlando FL, December 2001.

Chao RC, Teel L, Kogan SC, Shannon KM. Radiation induces a spectrum of myeloid malignancies in *Nf1* mutant mice. Selected for presentation at the 2001 Meeting of the American Society of Hematology, Orlando FL, December 2001.

(c) Model Development

The studies conducted to date have established a regimen for administering cyclophosphamide with and without radiation to F1 C56BL6/129Sv mice that should be useful for future studies of tumorigenesis and chemopreventive strategies in *Nf1* mice. The *Hprt* and protein truncation assays are generally applicable for mutation detection studies in *Nf1* mice.

(d) Employment and Research Opportunities

Richard Chao, M.D. is a fellow in adult hematology/oncology who has been supported by this award. Dr. Chao performed the radiation/cyclophosphamide studies, and has submitted a Mentored Physician-Scientist (K08) grant application to the NIH based on these preliminary data. He is interested in pursuing a career in translational research.

Brian Weiss, M.D. is a young pediatric hematology/oncology faculty member who has carried out the MM/MPA studies. He was recently awarded a KO8 from the National Cancer Institute.

Alfred Au, Zabi Wardak, Myla Sanchez, and Abigail Aiyagari are technical personnel in the investigator's laboratories who have received partial salary support from this award.

CONCLUSIONS

We have largely accomplished two of the three major goals of this translational research project. A thorough evaluation of MM in our *in vivo* model surprisingly demonstrated myeloid proliferation. This is consistent with case reports from a few human patients treated with this agent (21). While these *in vivo* data preclude the therapeutic use of MM this agent in JMML, they might underlie recent preliminary evidence that MM enhances hematopoiesis in some patients with MDS. Importantly, our biochemical analysis to date supports the idea that MM did decrease the activation state of the Ras effectors ERK and PKB in myeloid cells. These findings suggest that it might be feasible to blunt hyperactive Ras signaling in cells that have inactivated NF1 by lowering cellular GTP levels. Low dose treatment with MM might therefore merit preclinical evaluation in models of other NF1-associated complications. We are measuring Ras-GTP levels in cells exposed to MM, and will write a paper summarizing our data when this final set of experiments are completed.

By contrast, our experience with DT_{ct}GM-CSF has been frustrating. Dr. Perentesis successfully generated preparations that target the GM-CSF receptor; however, these were not cytotoxic. His laboratory has made substantial efforts to improve the methods used to produce DT_{ct}GM-CSF, and he is fully committed to continuing this work. Dr. Shannon will use alternative sources of funding to perform *in vitro* and *in vivo* testing of these newer preparations of DT_{ct}GM-CSF. Genetic evidence form our studies in *Nf1* and *Gmcsf* mutant mice and studies by others in xenograft systems strongly support the GM-CSF receptor as a valid target for therapeutic intervention in JMML (13, 22, 23).

Finally, our studies of the effects of RT and cyclophosphamide on cancer formation in heterozygous *Nf1* mutant mice have generated an large set of preliminary data and a valuable collection of cell lines and tumors for molecular and biochemical analysis. Clearly, exposure to these mutagens strongly potentiates the cancer predilection of *Nf1* mutant mice. Importantly, myeloid leukemia and sarcoma are the two most important second malignant neoplasms found in human patients with and without NF1 who are treated for cancer. The models we have developed therefore hold great promise for elucidating the pathogenesis of these cancers. Dr. Chao is currently sacrificing the last few mice in this cohort and is beginning an extensive set of molecular studies. We anticipate submitting a least two papers in 2002. Given the complex and long-term nature of these translational research studies, it is unfortunate that the U.S. Army NF Program does not support awards of > 3 years duration at this time.

References

1. **Maris JM, Wiersma SR, Mahgoub N, et al.** Monosomy 7 myelodysplastic syndrome and other second malignant neoplasms in children with neurofibromatosis type 1. *Cancer.* 1997;79:1438-46.

2. **Shannon KM, O'Connell P, Martin GA, et al.** Loss of the normal NF1 allele from the bone marrow of children with type 1 neurofibromatosis and malignant myeloid disorders. *N Engl J Med.* 1994;330:597-601.

3. **Kalra R, Paderanga D, Olson K, Shannon KM.** Genetic analysis is consistent with the hypothesis that *NF1* limits myeloid cell growth through $p21^{ras}$. *Blood.* 1994;84:3435-3439.

4. **Miles DK, Freedman MH, Stephens K, et al.** Patterns of hematopoietic lineage involvement in children with neurofibromatosis, type 1, and malignant myeloid disorders. *Blood.* 1996;88:4314-4320.

5. **Bollag G, Clapp DW, Shih S, et al.** Loss of *NF1* results in activation of the Ras signaling pathway and leads to aberrant growth in murine and human hematopoietic cells. *Nat Genet.* 1996;12:144-148.

6. **Side L, Taylor B, Cayouette M, et al.** Homozygous inactivation of the NF1 gene in bone marrow cells from children with neurofibromatosis type 1 and malignant myeloid disorders. *N Engl J Med.* 1997;336:1713-1720.

7. **Jacks T, Shih S, Schmitt EM, Bronson RT, Bernards A, Weinberg RA.** Tumorigenic and developmental consequences of a targeted *Nf1* mutation in the mouse. *Nat Genet.* 1994;7:353-361.

8. **Mahgoub N, Taylor B, Le Beau M, et al.** Myeloid malignancies induced by alkylating agents in Nf1 mice. *Blood.* 1999;93:3617-3623.

9. **Largaespada DA, Brannan CI, Jenkins NA, Copeland NG.** *Nf1* deficiency causes Ras-mediated granulocyte-macrophage colony stimulating factor hypersensitivity and chronic myeloid leukemia. *Nat Genet.* 1996;12:137-143.

10. **Zhang Y, Vik, TA, Ryder, JW, Srour, EF, Jacks, T, Shannon, K, Clapp, DW.** Nf1 regulates hematopoietic progenitor cell growth and Ras signaling in response to multiple cytokines. *J Exp Med.* 1998;187:1893-902.

11. **Allison AC, Waters RV.** Long-acting antirheumatic drugs induce differentiation of cells of the monocyte-macrophage lineage and alter the expression of cytokines and IL-1 receptor antagonist. *Agents Actions Suppl.* 1993;44:113-27.

12. **Eugui EM, Almquist SJ, Muller CD, Allison AC.** Lymphocyte-selective cytostatic and immunosuppressive effects of mycophenolic acid in vitro: role of deoxyguanosine nucleotide depletion. *Scand J Immunol.* 1991;33(2):161-73.

13. **Birnbaum RA, O'Marcaigh A, Wardak Z, et al.** Nf1 and Gmcsf interact in myeloid leukemogenesis. *Mol Cell.* 2000;5(1):189-95.

14. **DeClue JE, Heffelfinger S, Benvenuto G, et al.** Epidermal growth factor receptor expression in neurofibromatosis type 1- related tumors and NF1 animal models. *J Clin Invest.* 2000;105(9):1233-41.

15. **Mahgoub N, Taylor BR, Gratiot M, et al.** In vitro and In vivo effects of a farnesyltransferase inhibitor on Nf1- deficient hematopoietic cells. *Blood.* 1999;94(7):2469-76.

16. **Major IR, Mole RH.** Myeloid leukaemia in x-ray irradiated CBA mice. *Nature.* 1978;272(5652):455-6.

17. **Cichowski K, Shih TS, Schmitt E, et al.** Mouse models of tumor development in neurofibromatosis type 1. *Science.* 1999;286(5447):2172-6.

18. **Vogel KS, Klesse LJ, Velasco-Miguel S, Meyers K, Rushing EJ, Parada LF.** Mouse tumor model for neurofibromatosis type 1. *Science.* 1999;286(5447):2176-9.

19. **Meng Q, Skopek TR, Walker DM, et al.** Culture and propagation of Hprt mutant T-lymphocytes isolated from mouse spleen. *Environ Mol Mutagen.* 1998;32(3):236-43.

20. **Kataoka Y, Perrin J, Hunter N, Milas L, Grdina DJ.** Antimutagenic effects of amifostine: clinical implications. *Semin Oncol.* 1996;23 (suppl 8):53-57.

21. **Taylor DO, Ensley RD, Olsen SL, Dunn D, Renlund DG.** Mycophenolate mofetil (RS-61443): preclinical, clinical, and three-year experience in heart transplantation. *J Heart Lung Transplant.* 1994;13(4):571-82.

22. **Iversen P, Rodwell RL, Pitcher L, Taylor KM, Lopez AF.** Inhibition of proliferation and induction of apoptosis in JMML cells by the grnaulocyte-macrophage colony-stimulating factor analogue E21R. *Blood.* 1996;88:2634-2639.

23. **Iversen PO, Lewis ID, Turczynowicz S, et al.** Inhibition of granulocyte-macrophage colony-stimulating factor prevents dissemination and induces remission of juvenile myelomonocytic leukemia in engrafted immunodeficient mice. *Blood.* 1997;90(12):4910-7.

Draft Preview of Abstract #554355

DO NOT SIGN THIS COPY, THIS IS A DRAFT ONLY

Print

The 43rd ASH Annual Meeting

Presenting Author: Richard C Chao MD

Department/Institution: Dept. of Pediatrics, University of California at San Francisco

Address: Box 0519, 513 Parnassus Ave, HSE 302, San Francisco, CA 94143

City/State/Zip/Country: San Francisco, CA, 94143

Phone: (415) 476-5122 **Fax:** (415) 502-5127 **E-mail:** chao99@alumni.duke.edu

Presenting author is member of the American Society of Hematology: No

Presenting author is an Associate Member of ASH (member in training): No

Sponsoring Member: Kevin M Shannon

Department/Institution: Dept. of Pediatrics, University of California at San Francisco

Address: Box 0519, 513 Parnassus Ave., HSE 302

City/State/Zip/Country: San Francisco, CA, 94143

Phone: (415) 476-7932 **Fax:** (415) 502-5127 **E-mail:** kevins@itsa.ucsf.edu

Category: 632. Myelodysplastic Syndromes

Filename: 554355

Presentation format: No preference
Special consideration: No

Award: Post Doctoral Fellow
Payment type: Electronic

Radiation Induces a Spectrum of Myeloid Malignancies in *Nf1* Mutant Mice

Richard C Chao [1,3*], Lewis Teel [1*], Scott C Kogan [2] and Kevin M Shannon [1]. [1]Dept. of Pediatrics, University of California at San Francisco, San Francisco, CA, 94143, United States; [2]Dept. of Laboratory Medicine, University of California at San Francisco, San Francisco, CA, 94143, United States; and [3]Dept. of Medicine, Veterans' Affairs Medical Center, San Francisco, CA, 94121, United States.

Persons with neurofibromatosis type 1 (NF1) are predisposed to specific benign and malignant tumors, including juvenile myelomonocytic leukemia (JMML). Clinical observations suggest that individuals with NF1 may also be at increased risk of developing therapy-associated solid tumors and myeloid disorders after receiving chemotherapy and/or radiation (Maris, et al, *Cancer 79*:1438, 1997). In addition, heterozygous inactivation of murine *Nf1* cooperates with cyclophosphamide (CY) exposure in myeloid leukemogenesis (Mahgoub, et al, *Blood 93*:3617, 1999). We used F1 C57Bl/6 x 129/Sv heterozygous *Nf1* mutant mice (*Nf1* +/-) as a model to examine the effect of radiation alone and in combination with CY in the development of secondary myeloid disorders. A total of 104 wild-type and 85 *Nf1* +/- mice were assigned to one of four treatment groups: no treatment, CY 200 mg/kg/wk intraperitoneally x 6 doses, 3Gy irradiation, or sequential CY + radiation at these doses. All mice have been followed at least 14 months. CY and radiation, when given alone or in combination, produced reproducible leukopenia and anemia. Preliminary evaluation of the first 162 mice revealed 70 with a malignancy including 23 with malignant myeloid disorders. Other tumor types observed to date include sarcoma, pheochromocytoma, lymphoma, lung cancer, and Harderian gland tumors. None of 17 untreated wild-type mice developed a myeloid disorder, whereas 3/10 (30%) of control *Nf1* +/- mice developed disease. In radiation-treated mice, 4/24 (17%) wild-type versus 8/25 (32%) *Nf1* +/- animals developed myeloid disease. The number of *Nf1* +/- mice developing disease is probably underestimated, as four additional mice developed massive splenomegaly (>1g), but died without adequate necropsies. Including these mice increases the proportion of irradiated *Nf1* +/- with myeloid disorder to 48% of the cohort. Interestingly, myeloid malignancies were observed less frequently in mice that received CY alone or CY + radiation. The myeloid disorders detected in radiation-treated mice encompassed a broad phenotypic spectrum including hypoplasia, myeloproliferation, and myeloid leukemia, with varying degrees of dysplasia. Based upon the characteristics of myeloid disorders observed, including morphology, blood counts, bone marrow immunophenotype, spleen weight, tissue infiltration, and CFU-GM colony growth from bone marrow and spleen, we propose a classification scheme of secondary myeloid disorders that develop in mice. We are investigating if the myeloid disorders occurring in *Nf1* +/- mice are associated with loss of heterozygosity (LOH) at *Nf1* or with mutations in *Tp53*. These results demonstrate the utility of this murine model in studying secondary myeloid disorders. Our data are consistent with clinical

observations suggesting that NF1 patients are predisposed to radiation-induced secondary myeloid disorders, and provide evidence that radiotherapy should be avoided in treating NF1-associated tumors whenever possible.

Disclosure Statement:

Keywords:
myelodysplasia
therapy related leukemia
neurofibromatosis

Please select Print from the file menu to print your Abstract.

The 43rd ASH Annual Meeting

Presenting Author: Brian D Weiss MD
Department/Institution: Pediatrics, UC San Francisco
Address: HSE 302, Box 0519
City/State/Zip/Country: San Francisco, CA, 94143
Phone: (415) 514-4176 **Fax:** (415) 502-5127 **E-mail:** weissb@itsa.ucsf.edu
Presenting author is member of the American Society of Hematology: No
Presenting author is an Associate Member of ASH (member in training): No
Sponsoring Member: Kevin Shannon MD
Department/Institution: Pediatrics, UCSF
Address: HSE 302, Box 0519
City/State/Zip/Country: SF, CA, 94143
Phone: (415) 476-7932 **Fax:** **E-mail:** kevins@itsa.ucsf.edu
Category: 633. Myeloproliferative Syndromes
Filename: 554126

Presentation format: No preference
Special consideration: No

Award: Post Doctoral Fellow
Payment type: Electronic

Myeloproliferation in Wild-Type and *Nf1* Mutant Mice Treated With Mycophenolate Mofetil

Brian D Weiss [1*], Dan Lee [1*], Amy Feldmann [1*], Abby Aiyagari [1*] and Kevin Shannon [1]. [1]Pediatrics, UC San Francisco, San Francisco, CA, 94143, United States.

Mycophenolate mofetil (MM), also known as Cell Cept®, is commonly used to treat transplant rejection and has recently been studied as an antineoplatic agent. Its active moiety, mycophenolic acid (MPA), competitively inhibits inosine monophosphate dehydrogenase (IMPDH), thereby leading to depletion of the GTP pool in certain cell types. Since Ras activation depends on GTP binding, therapeutics that lower the ratio of GTP to GDP could potentially inhibit Ras-dependent growth. Purines (e.g. guanine, adenosine) can be synthesized either *de novo* or via the salvage pathway. While most cell types can utilize both pathways, lymphocytes and (possibly) monocytes can only assemble guanine *de novo* ; thus, inhibiting IMPDH depletes guanine and the GTP pool. Previous *in vitro* studies found that 1-10 μM MPA depleted GTP in human lymphocytes and monocytes but not in neutrophils. Conversely, concentrations of MPA up to 10 μM had no effect on neutrophil chemotaxis, superoxide burst, or bacteria-killing ability. We have initiated a study of MM in a Ras-GTP dependent neoplastic model. Mice homozygous for a mutation at *Nf1* (*Nf1* -/-) die *in utero* ; however, irradiated hosts transplanted with *Nf1* -/- hematopoietic progenitors survive and develop a myeloproliferative disorder that models juvenile myelomonocytic leukemia (JMML) (Largaespada et al, Nat Genet, 1996). Features of this disease include splenomegaly with myeloid invasion, leukocytosis, and granulocyte macrophage-colony stimulating factor (GM-CSF) hypersensitivity. Recipient mice repopulated with wild-type (*Nf1* +/+) or *Nf1* -/- hematopoietic cells were treated with 400 mg/kg of MM each day with the hopes of modulating the disease phenotype via depletion of the GTP pool. Unexpectedly, MM treatment was associated with profound blood leukocytosis and neutrophilia. In mice engrafted with *Nf1* +/+ fetal liver cells, white blood cell (WBC) counts increased from 7,000±1,500 cells/μl to 26,500±6,500 cells/μl with MM exposure. Similarly, WBC counts of *Nf1* -/- recipients rose from 28,000±4,000 cells/μl to 74,000±28,000 cells/μl after treatment. These data are consistent with rare case reports of leukocytosis and neutrophilia in patients treated with MM (Taylor et al, J Heart Lung Transplant, 1994). Furthermore, MM treatment was associated with an increase in the spleen weight and the number of colony forming units-granulocyte macrophage (CFU-GM) per spleen in mice of both genotypes. Preliminary biochemical studies revealed that MM had no effect on basal or GM-CSF induced ERK kinase activity while paradoxically reducing Akt activity in bone marrow mononuclear cells. We are continuing to interrogate GTP-dependent signaling pathways in primary cells.

Disclosure Statement:

Keywords:
mycophenolate mofetil
myeloproliferation
neurofibromatosis

Signatures

An ASH member must sign the abstract form. The member's signature certifies the member's understanding of the following rules for participation in the ASH meeting: (1) All authors approve submitting this work for presentation; (2) The author(s) transfer(s) all copyright ownership of the named abstract to the American Society of Hematology; (3) All authors have read the ASH Abstract Disclosure Policy and have acted in accordance with that policy; (4) The author(s) agree(s) to materially confine the presentations to information in the abstract if accepted for presentation. If an author has more than one abstract accepted, each presentation will be materially confined to the information in the abstract selected for the specific session; (5) At least one author will be available to present the abstract if selected for the program. The author(s) will immediately notify ASH if they are unable to present an abstract or if the presenting author is changed; and (6) The data in the abstract are not expected to be published prior to the time of the presentation, nor will they be materially presented at another national meeting or on Corporate Friday prior to the ASH meeting.

Signature of Presenting Author or Sponsoring Member
(if the Presenting Author is not a American Society of Hematology member):

Kevin Shannon MD

Return To Thank You

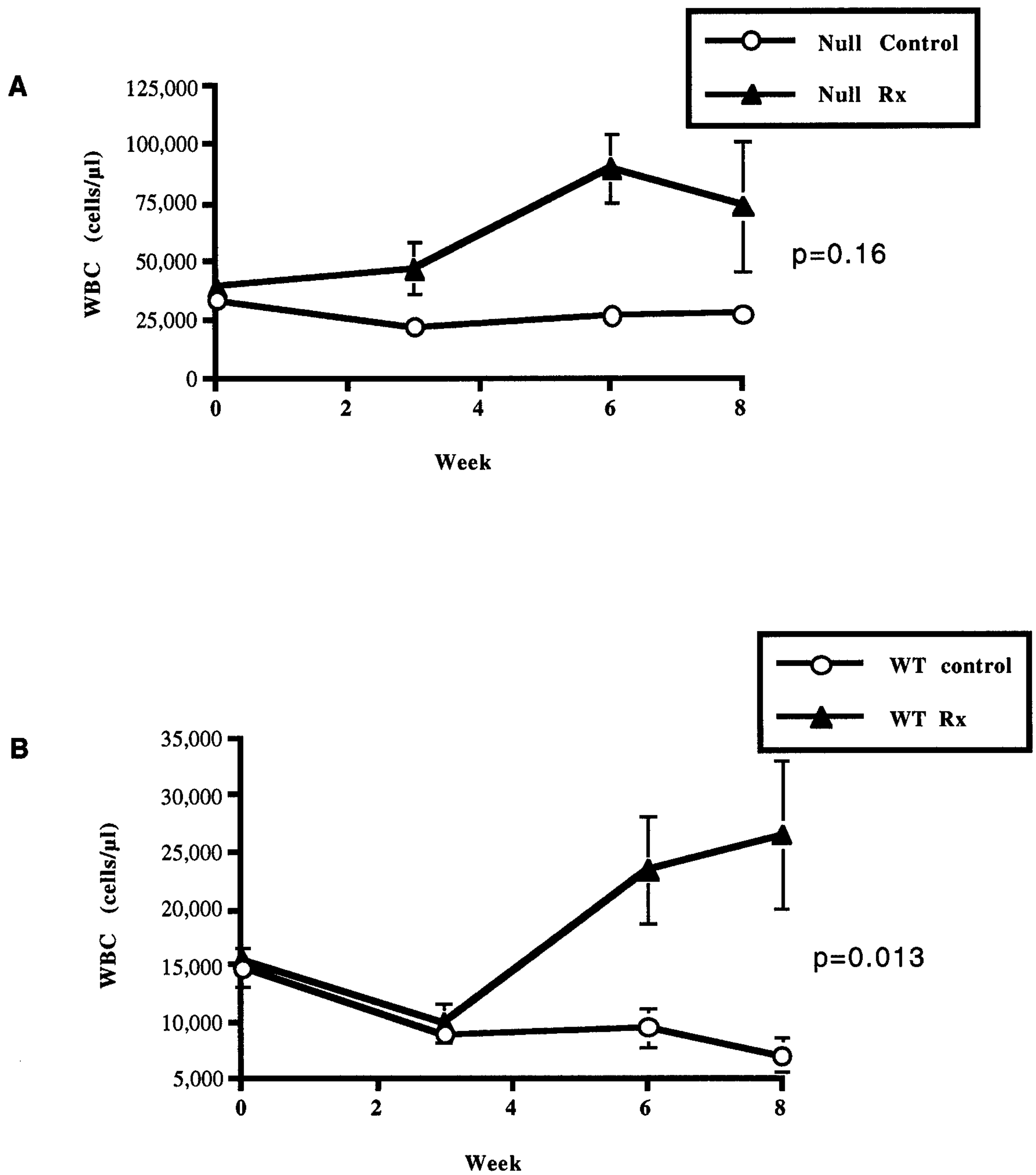

Figure 1. Effect sof MM Treatment on White Blood Cell Counts in Mice Engrafted with *Nf1-/-* (panel A) or *Nf1+/+* (panel B) Fetal Liver Cells. Control mice were treated with sterile vehicle and "Rx" mice were treated with 400 mg/kg/day of MM daily for 8 weeks. Note that baseline white blood cell counts were much higher in recipients of *NF1-/-* cells. The increase in WBC was due to a rise in myeloid cells in both groups of Rx mice.

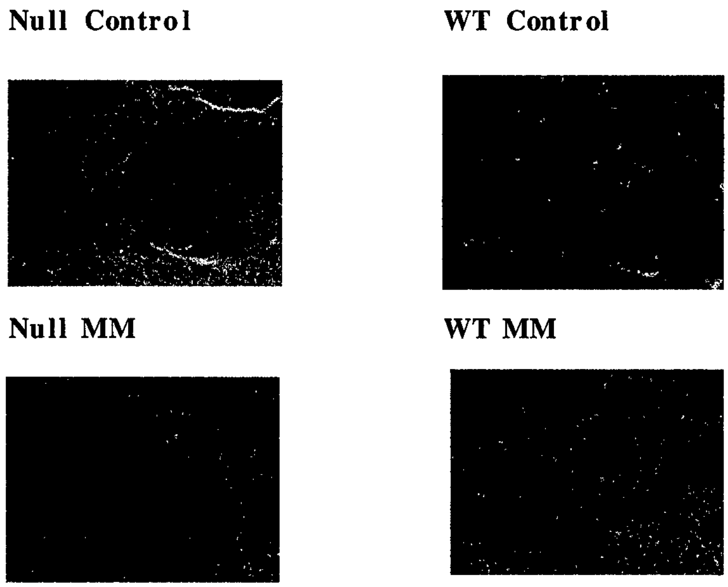

Figure 2. Effects of MM Treatment on Splenic Morphology. Mice transplanted with Wild-Type (WT) or *Nf1-/-* cells were treated with 8 weeks of either sterile control vehicle or MM at 400mg/kg/day. WT spleen has normal morphology after control treatment but shows evidence of massive myeloid invasion after MM treatment. Similarly, while Null spleen shows mild myeloid invasion at baseline, MM treatment greatly increases the myeloid content of the spleen and disrupts normal splenic architecture.

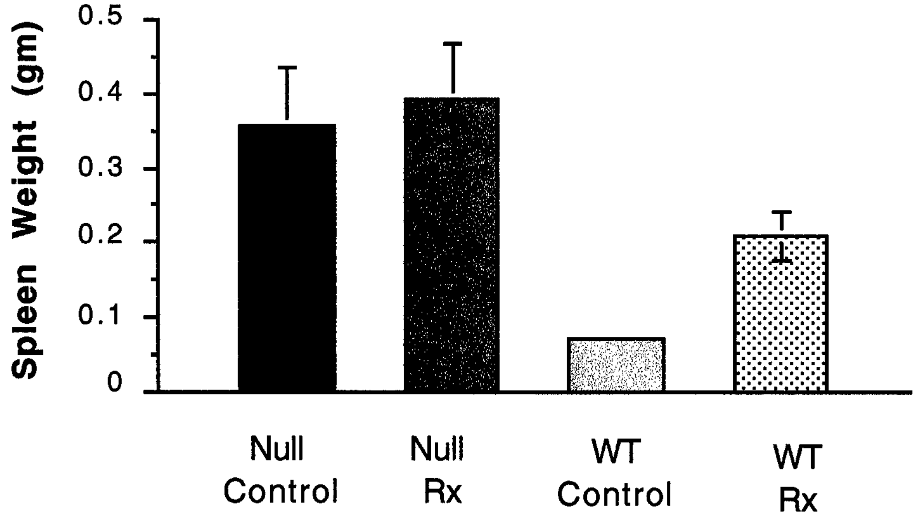

Figure 3. Spleen Weights in Recipient Mice Engrafted with *Nf1-/-* ("null") or Wild-Type (WT) Fetal Liver Cells. Control mice were treated with sterile vehicle and "Rx" mice were treated with 400 mg/kg/day of MM daily for 8 weeks. *Nf1-/-* ("null") recipients treated with MM did not have a significantly larger spleens than *Nf1-/-* controls (p=0.8). On the other hand, *Nf1+/+* recipients exposed to MM had significantly larger spleens than *Nf1+/+* controls (p<0.05), and in fact had a mean splenic weight which approached that of MM-treated *Nf1-/-* mice (p=0.9).

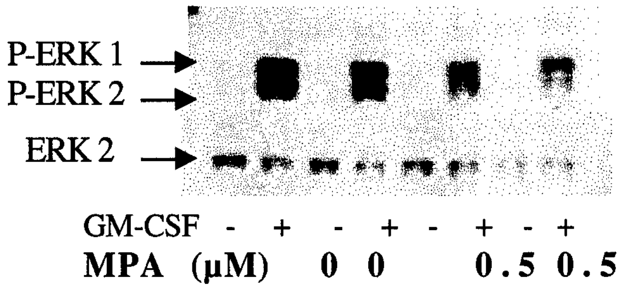

Figure 4. Effects of MPA on Phosphorylated-ERK Levels in *Nf1-/-* and WT Murine *Myb* Lines Generated from Fetal Liver Cells. Cells were starved of GM-CSF for 4 hours while incubated with varying concentrations of mycophenolic acid (MPA) at 37°C. Samples were then split and incubated at 37°C with either 10 ng/mL of recombinant murine GM-CSF or blank for 7.5 minutes. Cell lysates were run on an 8% TGS gel then transferred to filter paper. Blots were then probed with a polyclonal antibody against Phospho-ERK and a polyclonal anti-ERK2 antibody as a control. MPA at increasing concentrations appears to block the ability of upstream effectors (e.g Ras) to phosphorylate ERK in response to GM-CSF stimulation.

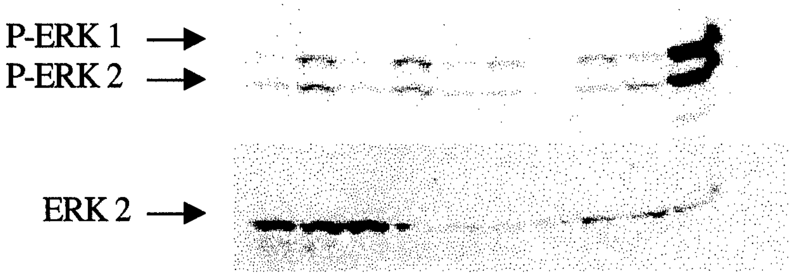

Mouse	A	A	B	B	C	C	D	D	E	E
GM-CSF	-	+	-	+	-	+	-	+	-	+
MM	0	0	0	0	+	+	+	+	+	+
Time	4	4	4	4	4	4	4	4	24	24

Figure 5. Effects of MM Treatment on ERK Activation. *Nf1* +/- mice were treated daily for 6 days with 400 mg/kg of MM per day. Mice were sacrificed 4 and 24 hours after the final dose of MM and their bone marrows were harvested with minimal handling. Bone marrow cells were incubated at 37°C with either 10 ng/mL of recombinant murine GM-CSF or blank for 7.5 minutes. Cell lysates were run on an 8% TGS gel then transferred to filter paper. Blots were then probed with a polyclonal antibody against Phospho-ERK and a polyclonal anti-ERK2 antibody as a control. MM appears to block the ability of upstream effectors (e.g. Ras) to phosphorylate ERK in response to GM-CSF. This effect has dissipated by 24 hours, and a rebound hyperstimulation can be seen.

P-GSK-3b

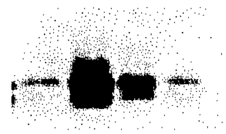

Mouse	F	F	G	G
GM-CSF	-	+	-	+
MM	0	0	+	+
Time	4	4	4	4

<u>Figure 6.</u> Effects of MM Treatment on PKB Activation. *Nf1* +/+ mice were treated daily for 6 days with 400 mg/kg of MM per day. Mice were sacrificed 4 hours after the final dose of MM and bone marrow was harvested with minimal handling. Bone marrow cells were incubated at 37°C with either 10 ng/mL of recombinant murine GM-CSF or blank for 7.5 minutes. PKB/Akt was immunoprecipitated by incubating cell lysates with anti-PKB beads overnight. GSK-3b fusion protein was added to sample and incubated for 30 minutes at 30°C. Samples were run on a 10% TGS gel then transferred to filter paper. The ability of PKB to phosphorylate GSK-3b fusion protein was evaluated with anti-phospho-GSK-3b antibody. MM appears to block the ability of upstream effectors such as Ras to activate PKB, which then phosphorylates GSK-3b, in response to GM-CSF stimulation.

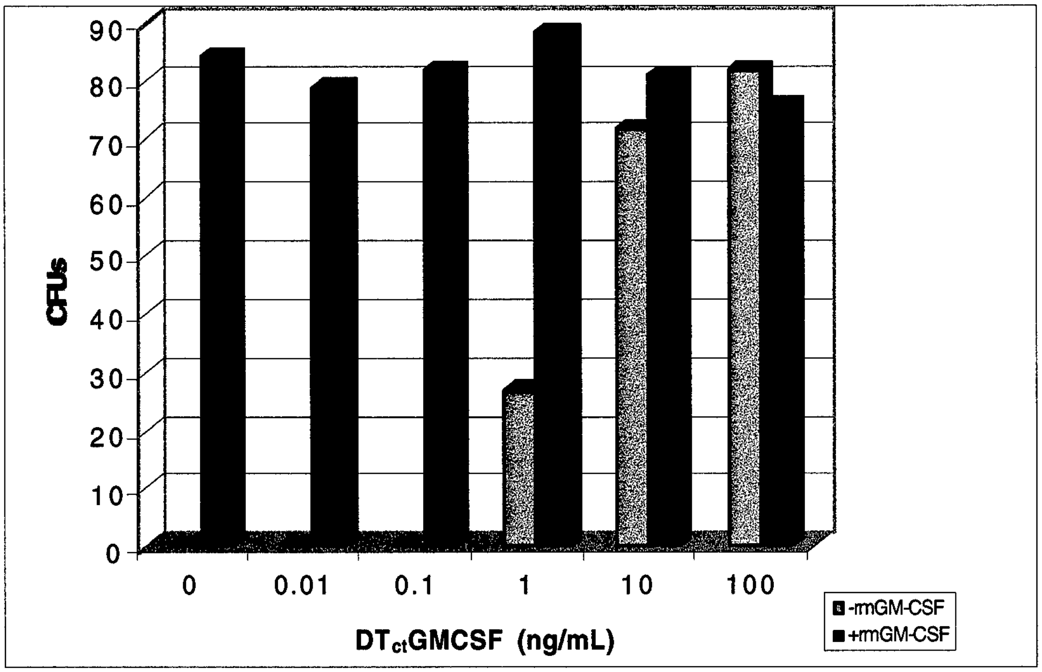

Figure 7. Effects of DT_{ct}GM-CSF on CFU-GM Colony Growth from Normal Mouse Bone Marrow. Marrow mononuclear cells were plated in methylceullulose medium containing various concentrations of DT_{ct}GM-CSF in the presence or absence of GM-CSF as shown. DT_{ct}GM-CSF did not anatagonize colony growth at any concentration tested, and showed agonist activity at 1 ng/mL and above.

DT-mGMCSF Transformed HMS174(de3)plysS
OD=0.6
⇓
IPTG-INDUCED CULTURE (1 HR)
⇓
⇒ SUPERN/
PELLET
⇓
LYSIS (Tris/EDTA/1%Triton X) + Lysozyme (30°C, 15 min)
⇓
SONICATE + Protein inhibitor cocktail
⇓
10,000g
⇓
⇒ SUPERN/
PELLET ---- INCLUSION BODIES
(WASH 2X)
⇓
SOLUBILIZATION (CAPS/N-Lauroylsarcosine/DTT) 15 min R.T
⇓
10,000g
⇓
⇒
SUPERNATANT
⇓
DIALYSIS against REFOLDING BUFFER (TRIS/ +/- DTT / Na CL+/- NDSB)
4°C 48HR
⇓
10,000g
⇓
⇒
SUPERNATANT
⇓
SEPHAROSE (0.3M NaCl)

Figure 8. DT-mGMCSF Expression and Purification Methods for Improved Renaturation Refolding of DT-mGMCSF.

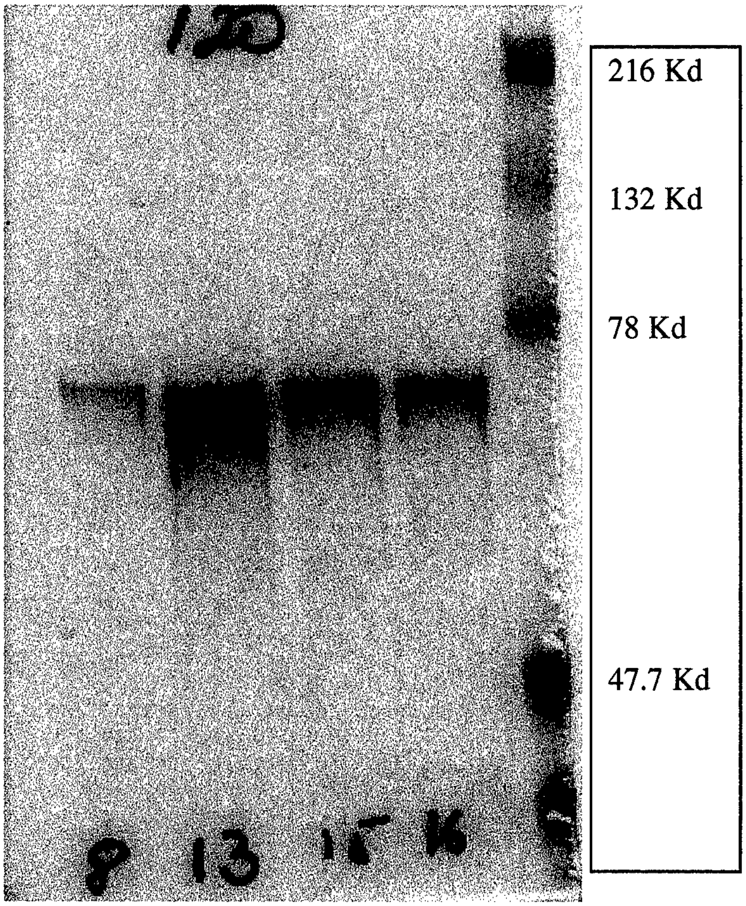

Figure 9. Analysis of different methods for improved DT-mGMCSF recombinant fusion toxin expression and renaturation. High yield column fractions from isolation #120 shown.

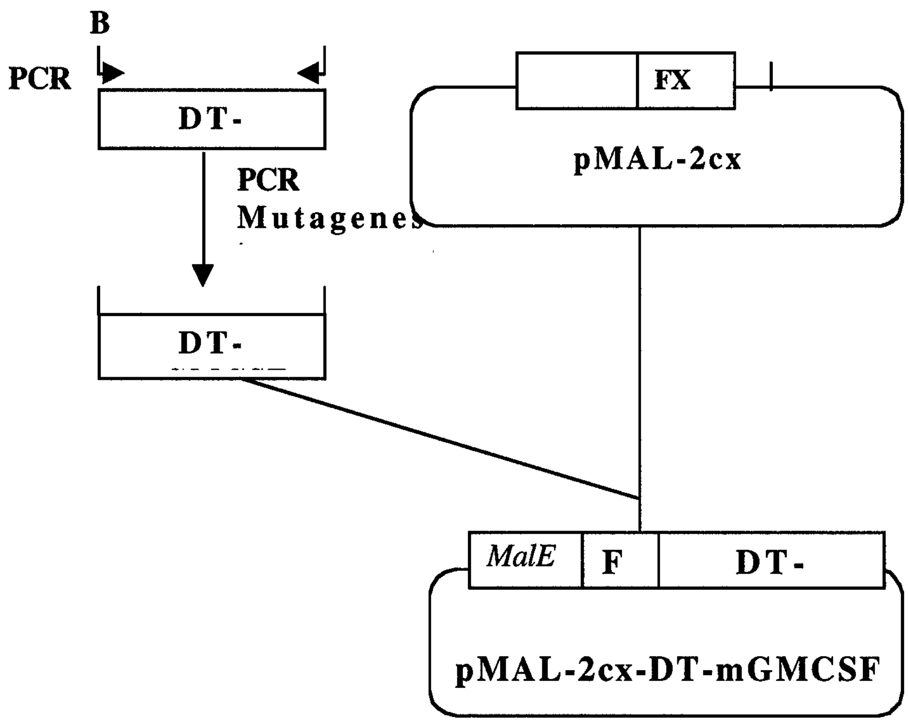

Figure 10. Overview of the construction of expression vector pMAL-2cx-DT-mGMCSF (see text for details).

E. coli with Expression Vector - OD ≈ 0.5-0.8

↓

IPTG to final conc. 0.3-0.5 mM

↓

Transfer culture to low temperature

[15°C → O/N
| 20-25°C → O/N
[30°C → 6 hours]

↓

Cell harvest at 5000 g for 10 min at 4°C

Pellet stored at -20°C, or resuspended in 50 ml ice cold cell lysis buffer -- 20 mM Tris-Cl pH 8.0

500 mM NaCl
1 mM EDTA or 0.1%
Triton X-100 or Tween 20
PMSF

↓

Sonication → 2 min (1 min pulses)

|→ Total cell extract → SDS sample

↓

Centrifuge at 20,000 xg for 30 min at 4°C

↙ ↘

Supernatant (soluble cell extract) | Pellet (insoluble cell extract)

↓→ SDS sample

Load onto chitin column at flow rate 0.5-1 ml/min

↓

Collect the flow through

↓→ SDS sample

Wash column with high flow rate and stringent wash condition (>10x column volumes)

↓

Induce on column cleavage by quickly flushing the column with 3 bed volume of cleavage buffer 20 ~~mM~~ Tris-cl pH 8.0

200 mM NaCl
1 mM EDTA
50 mM cysteine
1 mM DTT

within 30 min. Stop the flow and left column at (1) 4°C for O/N (16-40 hours) → PTYB2-

(2) 16°C-23°C for 40 hours → PTYB12-

↓

Elute protein with column buffer

↓

Fractions collected → PAGE Analysis

Remove 200 μl of resin and mix with 100 μl SDS-sample buffer boiling and spin resin down

↓

Supernatant → SDS-sample

*Regeneration of chitin column: wash column with 3 bed volumes of 0.3 M NaOH → soak for 30 min

↓

wash again with 7 bed volumes of 0.3 M NaOH

↓

wash with 20 bed volumes dH20

↓

wash with 5 bed volumes column buffer

↓

Store at 4°C with 0.02% sodium azide in column buffer

Figure 11. Overview of the Expression and Purification of DT-mGMCSF from Expression Plasmids.

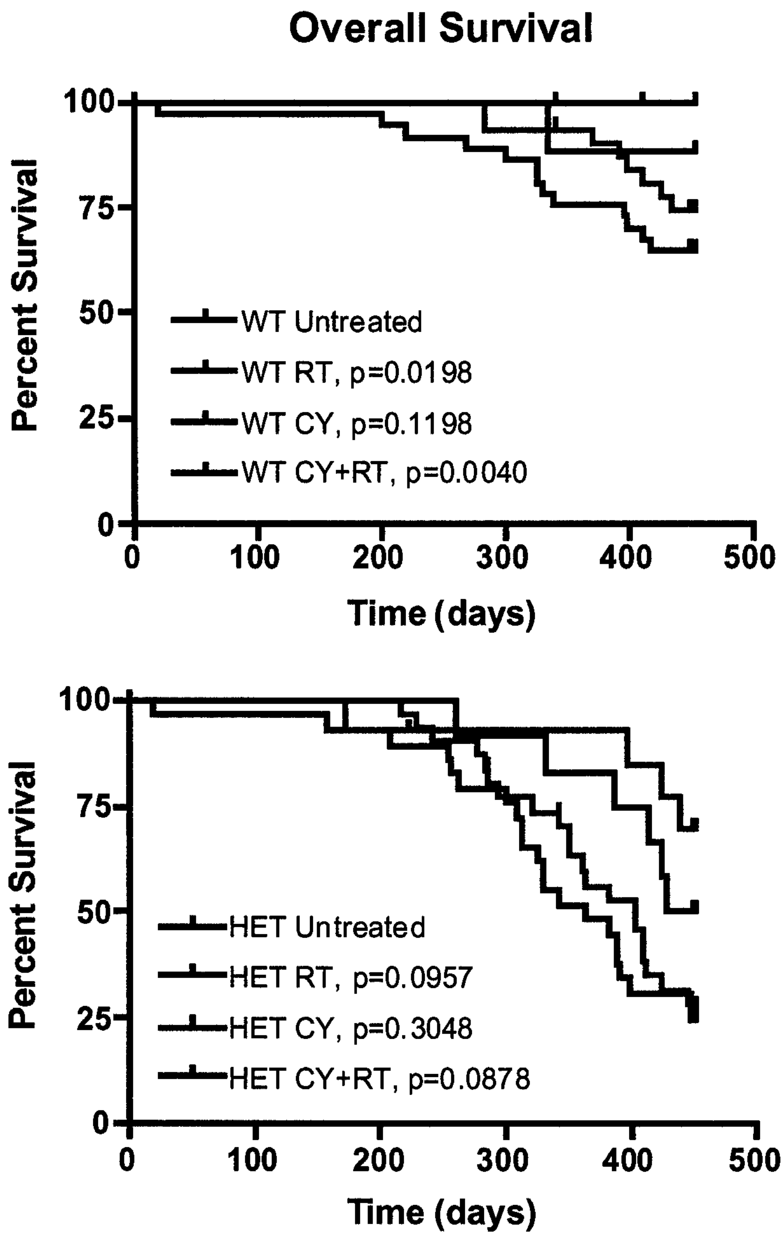

Figure 12. Kaplan-Meier Survival Analysis of Wild-Type (WT) and Heterozygous *Nf1* Mutant (HET) Mice Assigned to Various Treatment Groups. Mice are sacrificed at the time of excess morbidity or following the completion of a 15 month observation period after treatment. RT alone or in combination with CY increased the risk of death, although this does not reach statistical significance in the *Nf1*+/- mice. Additionally, *Nf1*+/- mice have an increased risk of death when compared to wild-type mice receiving the same treatment in the untreated, RT exposed, or CY+RT exposed groups but not in the CY treated groups. Panel A depicts survival for wild-type mice and Panel B depicts survival of *Nf1*+/- mice. Plots begin after the completion of all treatment.

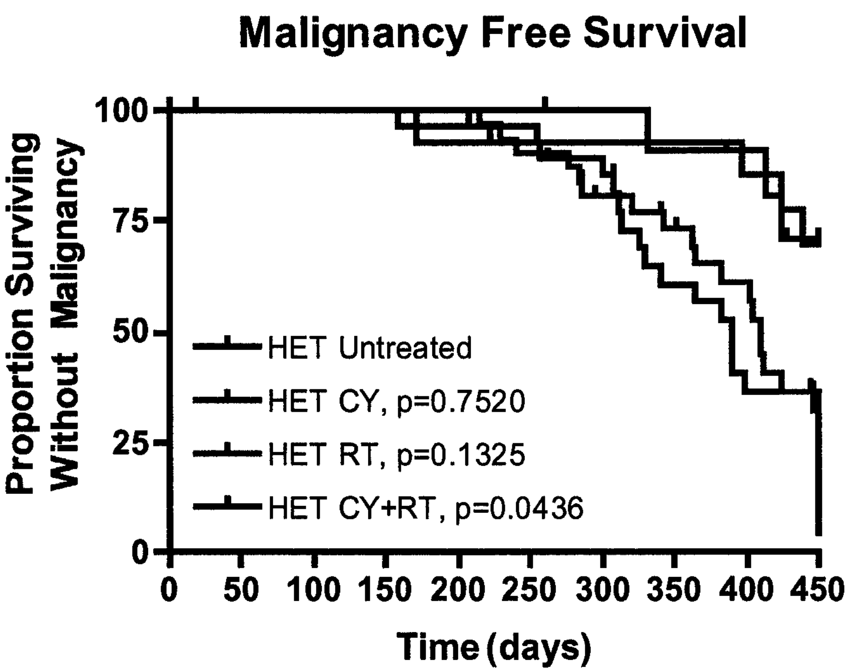

Figure 13. Kaplan-Meier Survival analysis of *Nf1+/-* (HET) mice demonstrates that CY+RT cooperates in the development of malignancy. Furthermore, CY+RT increases the risk and decreases the latency of development of a cancer when compared with CY only (p=0.0487).

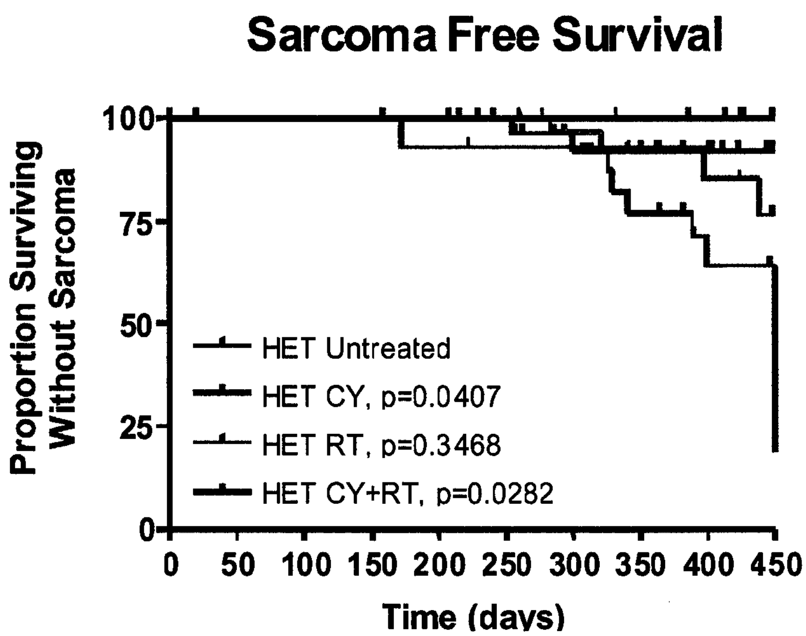

Figure 14. Kaplan-Meier curves showing survival without sarcoma development in *Nf1*+/- (HET) mice. None of the wild-type developed sarcomas regardless of treatment group (data not shown). In addition, none of the untreated *Nf1*+/- mice developed sarcomas. CY and CY+RT resulted in a significantly greater risk of developing sarcoma when compared to untreated controls. (p values by logrank comparing each treatment arm with the untreated, control arm).

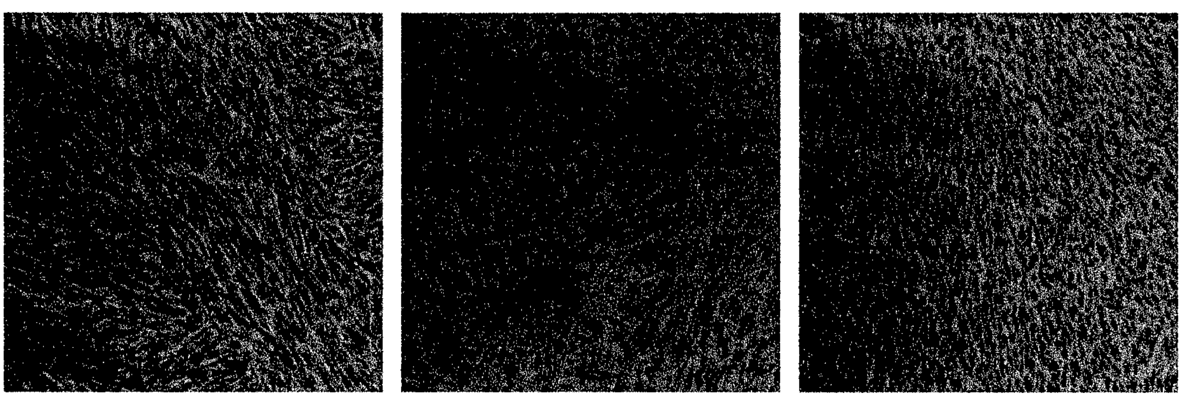

Figure 15. Sarcomas from in *Nf1*+/- Mutant Mice. Hematoxylin and eosin staining of tumor masses in mice exposed to CY (Panel A), RT (Panel B), and CY+RT (Panel C) reveal soft tissue sarcomas, displaying fascicles of spindle shaped cells with frequent mitotic figures. Panel A demonstrates a typical herringbone pattern while Panel B displays an area of central necrosis, both of which are characteristic of sarcomas.

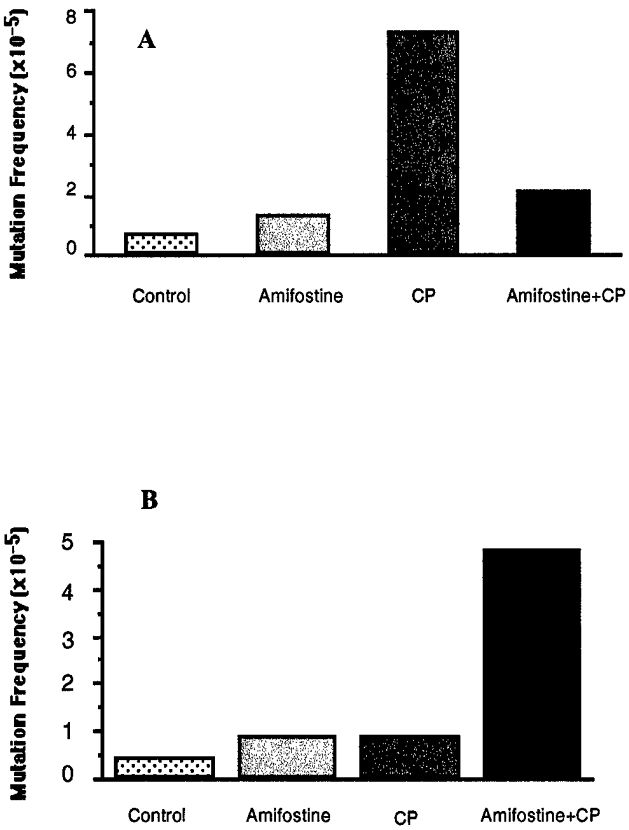

Figure 16. F1 129/Sv x C57Bl6 *Nf1+/-* mice ages 2-4 months received either a single dose (A) or 6 weekly doses (B) of amifostine at 200 mg/kg or control (sterile saline) by intraperitoneal injection 30 minutes prior to being injected intraperitoneally with either CY at 200 mg/kg or sterile water. Mice were sacrificed at 55-60 days and splenocytes were harvested. In mice treated for one week (A), control treated mice had a *Hprt* mutation frequency of 7×10^{-6} compared to 7×10^{-5} in CY-treated mice. Mice treated with amifostine + CY had a mutation frequency of 2×10^{-5}, approximately 70% less than mice treated with CY alone. In mice treated for 6 weeks (B), control treated mice had a *Hprt* mutation frequency of 4×10^{-6} compared to approximately 9×10^{-6} in CY-treated and amifostine-treated mice. Mice treated with amifostine + CY had a mutation frequency of almost 5×10^{-5}, 5 times that of CY alone.